

Solar Cells and Light Sensors Based on Nanoparticle-Grafted Carbon Nanotube Films

Xianglong Li,[†] Yi Jia,[‡] Jinquan Wei,[‡] Hongwei Zhu,[‡] Kunlin Wang,[‡] Dehai Wu,[‡] and Anyuan Cao^{§,*}

[†]Department of Mechanical Engineering, University of Hawaii at Manoa, Honolulu, Hawaii 96822, [‡]Key Laboratory for Advanced Materials Processing Technology, Ministry of Education, Department of Mechanical Engineering, Tsinghua University, Beijing 100084, China, and [§]Department of Advanced Materials and Nanotechnology, College of Engineering, Peking University, Beijing 100871, China

ABSTRACT Carbon nanotubes show great potential in developing solar cells with enhanced power conversion efficiency, yet the device stability has not been thoroughly studied. Here, we show how the interaction between components in a nanotube-based hybrid solar cell could cause a significant change in output voltage and fill factor, resulting in photoinduced degradation in device performance. We functionalized carbon nanotubes with CdS nanoparticles to make hybrid films and deposited these films onto silicon substrates to construct solar cells with efficiencies up to 1.4%. The $I-V$ characteristics show reversible change in response to light illumination, suggesting potential applications as visible-light sensors. The fill factor and open-circuit voltage gradually decrease under continuous illumination, inversely proportional to the incident light energy within a considerable range up to 60 J. The unique photoresponse is attributed to a charge-transfer process between nanotubes and nanoparticles under excitation and to change in series resistance in the solar cells.

KEYWORDS: hybrid · carbon nanotubes · nanoparticles · solar cell · charge transfer

Attaching nanoparticles to the surface of carbon nanotubes has been considered as a general strategy toward structural modification, morphology control, and construction of innovative architectures or heterostructures.^{1,2} The nanoparticles are either directly grown on the nanotube surface or connected to nanotubes by chemical functionalization, creating a wide range of hybrid materials with tailored interaction (e.g., covalent or non-covalent) between their components.^{1–5} Hybrids incorporating many different metallic and semiconducting nanoparticles have been reported recently, in which the morphology and distribution of nanoparticles can be reasonably controlled.^{4–10} These hybrid materials show promising applications in catalysis, sensors, and optoelectronic devices.^{11–16} For example, fuel cell electrodes containing well-dispersed Pt nanoparticles on multiwalled nanotubes result in higher electrocatalytic activity and stability than commercial Pt nanoparticles on carbon black.¹¹ CdSe–nanotube hybrids are capable of light-induced charge trans-

fer and can be used as an electron transport component in solar cells.¹⁶

There is a lot of interest in making bulk heterojunction solar cells by incorporating carbon nanotubes and their hybrid structures into conjugated polymers.^{17–20} Among these, attaching quantum dots onto nanotubes with matching band gap is considered as a potential way to enhance light absorption and charge dissociation.^{19,20} A major problem with this type of hybrid solar cells is that charge transfer and redistribution occur under light excitation, which often dominates the device performance. For example, the interface between metallic nanotubes and conjugated polymer is found to be unfavorable for exciton dissociation, which limits cell efficiency.²¹ If nanotube–nanoparticle hybrid structures are incorporated into photovoltaic devices, light-induced charge transfer is a critical process that needs to be considered. In many instances, nanotube networks can serve as electron acceptors from the excited CdS quantum dots, which results in detectable photocurrent through the nanotube device.^{3,16} Investigation on the electronic interaction between nanostructures in hybrid systems could facilitate development of next-generation solar cells.

Recently, we reported heterojunction solar cells by depositing a thin film of double-walled carbon nanotubes (DWNTs) onto a silicon substrate with power conversion efficiencies in the range of 1–7%.^{22,23} The energy band diagram across the heterojunction is favorable for charge carrier separation, resulting in efficient hole transport through the DWNT films and electron flow through the silicon side.²³ Here, we grafted cadmium sulfide (CdS) nanoparticles onto single-walled nanotubes

*Address correspondence to anyuan@pku.edu.cn.

Received for review November 5, 2009 and accepted March 3, 2010.

Published online March 11, 2010.
10.1021/nn901563y

© 2010 American Chemical Society

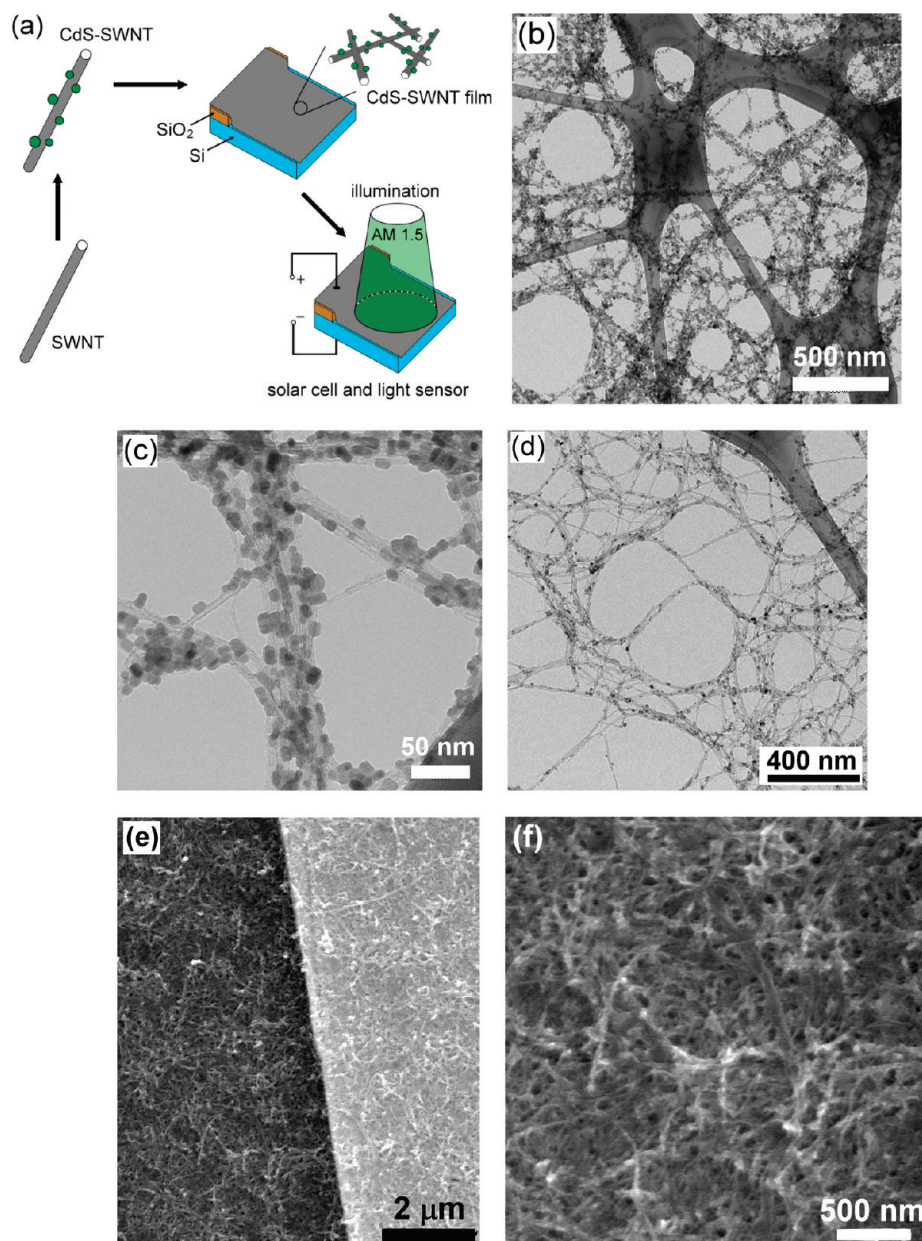


Figure 1. Fabrication of CdS–SWNT hybrid materials, solar cells, and light sensors. (a) Illustration showing the device fabrication process (see arrows) consisting of functionalization of SWNTs with CdS nanoparticles, deposition of the hybrid films onto silicon substrate, and the configuration of solar cells and light sensors in which the CdS–SWNT film connects to positive electrode (conducting holes) and the n-type silicon serves as the negative electrode (conducting electrons). (b) TEM image of CdS-grafted SWNT networks with 85.7 wt % CdS nanoparticles. (c) Higher magnification TEM image of the hybrid materials consisting of SWNT bundles and dispersed CdS nanoparticles. (d) TEM image of CdS–SWNT hybrids with 50 wt % nanoparticles. (e) SEM image of a solar cell showing the CdS–SWNT hybrid film deposited on a patterned Si/SiO₂ wafer (the white background region is SiO₂). (f) Top morphology of the CdS–SWNT film showing interconnected bundles.

(SWNTs) and made CdS–SWNT–Si heterojunction solar cells with efficiencies greater than 1%. Furthermore, we observed significant degradation of solar cell performance under light illumination due to introduction of CdS nanoparticles into SWNT films. The I – V characteristics and typical parameters of solar cells, such as fill factor (FF) and open-circuit voltage (V_{oc}), show reversible change during illumination followed by storage in the dark. Previously, hybrid CdSe–SWNTs were incorporated into organic solar cells with limited efficiency,¹⁹ and later a model was proposed based on SWNTs fully

covered by CdSe,¹⁶ yet a device with tunable FF and/or V_{oc} has not been reported.

The fabrication of solar cell devices and light sensors involves three basic steps, as shown in Figure 1. First, SWNT arrays grown by chemical vapor deposition (purity >99%) were dispersed into toluene with 0.1 vol % oleylamine by sonication and functionalized with CdS nanoparticles synthesized through a solution process (see details in our recent publication²⁴). The addition of a small amount of oleylamine is critical for obtaining stable hybrid materials with strong adhesion between

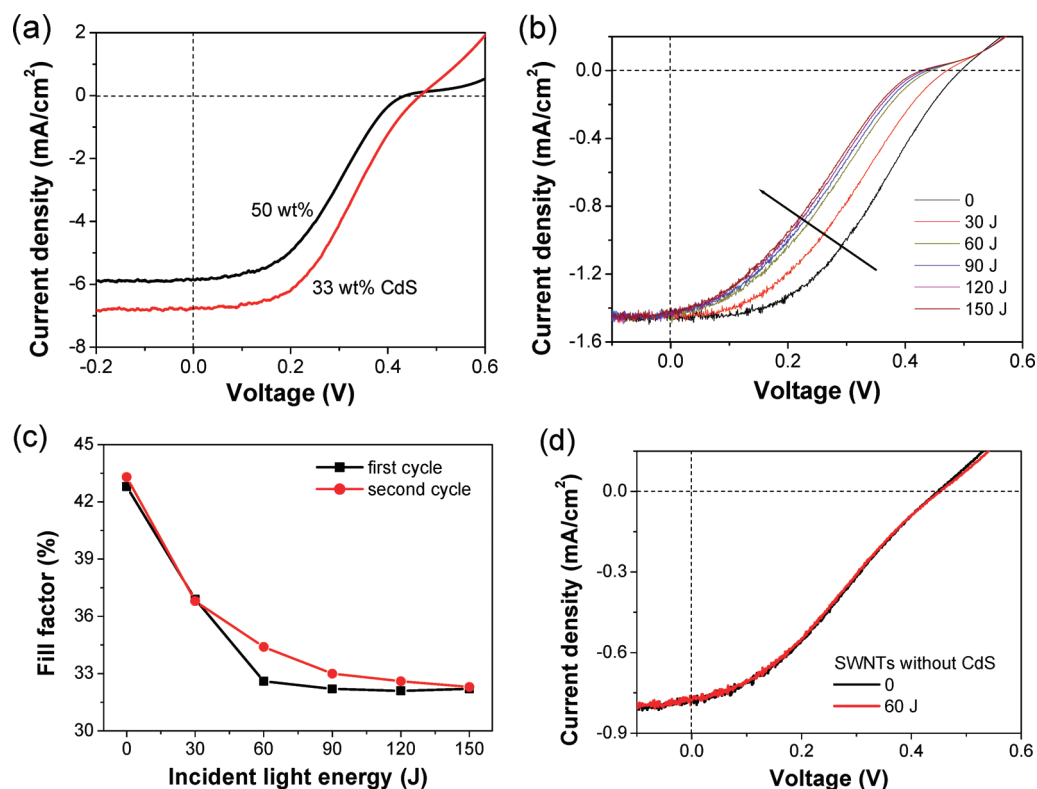


Figure 2. Characterization of solar cells and light sensors under illumination. (a) *I–V* characteristics of two solar cells containing different CdS weight percentages (50 and 33 wt %). (b) *I–V* characteristics of a solar cell under continuous illumination in which repeatedly collected curves were plotted at a time interval of 10 min (corresponding to an accumulated incident light energy of 30 J based on a device area of 0.5 cm² and incident light power of 100 mW/cm²). (c) Plots of fill factors after different illumination time (incident light energy) showing reversible change in two illumination cycles. After 50 min illumination (the first cycle), the cell was placed in the dark and air for 6 h until its fill factor recovered to its original value, and then illuminated for 50 min again (second cycle). (d) *I–V* characteristics of a control sample based on pristine SWNTs showing no change of typical parameters (V_{oc} , I_{sc} , FF) under long time illumination.

CdS and SWNTs. At the same time, noncovalent functionalization ensures minimum modification to the electronic properties of SWNTs. Second, semitransparent CdS–SWNT thin films were made by vacuum filtration with controlled film thickness (100 nm to 1 μ m) and then transferred to a n-type silicon substrate as a conformal coating. Third, solar cell devices were made by connecting electrodes to the SWNT film (positive) and Si substrate (negative). The electrical contact to SWNTs was made on a 300 nm thick oxide layer to prevent circuit shortage. The device performance and photoresponse were measured under uniform AM 1.5G illumination at a calibrated power intensity of 100 mW/cm².

Transmission electron microscopy (TEM) characterization shows a uniform attachment of CdS nanoparticles on oleylamine-functionalized SWNTs (Figure 1b,c). The diameters of CdS nanoparticles observed were between 5 and 10 nm, roughly the same size of the SWNT bundles. Separated CdS nanoparticles are grafted onto a single or small bundle of SWNTs without forming larger size agglomerates (Figure 1c). Good SWNT–nanoparticle adhesion was obtained because the nanoparticles remain on the SWNTs after more than 30 min bath sonication. The density and surface cover-

age of the hybrids can be controlled by the weight percentage of CdS (from 33 to 90 wt %) loaded during the functionalization.²⁴ For making solar cells, a modest loading (<50 wt %) was used because the presence of too much CdS nanoparticles may prevent SWNT interconnection and reduce film conductivity. A loading of 50 wt % CdS yields relatively lower surface coverage (<10%) on SWNTs (Figure 1d).

Solar cells are made by depositing CdS–SWNT hybrid films or SWNT films (as control sample) on a patterned silicon wafer (see Experimental Section). Scanning electron microscopy (SEM) characterization shows that CdS-grafted SWNT bundles form a two-dimensional, interconnected film conformally coated on both Si (active area) and SiO₂ regions (for insulation) (Figure 1e,f). The CdS nanoparticles present among the film cannot be clearly resolved here. The hybrid film is sufficiently thin to ensure that the incident light could reach the SWNT–Si interface to produce charge carriers from crystalline Si. The SWNTs in the hybrid film form heterojunctions with Si and extract and transport charge carriers (holes) like a transparent electrode. Here, the CdS–SWNT–Si cell is more complex than the DWNT–Si model we studied before²³ because some CdS nanoparticles may contact the Si substrate as well

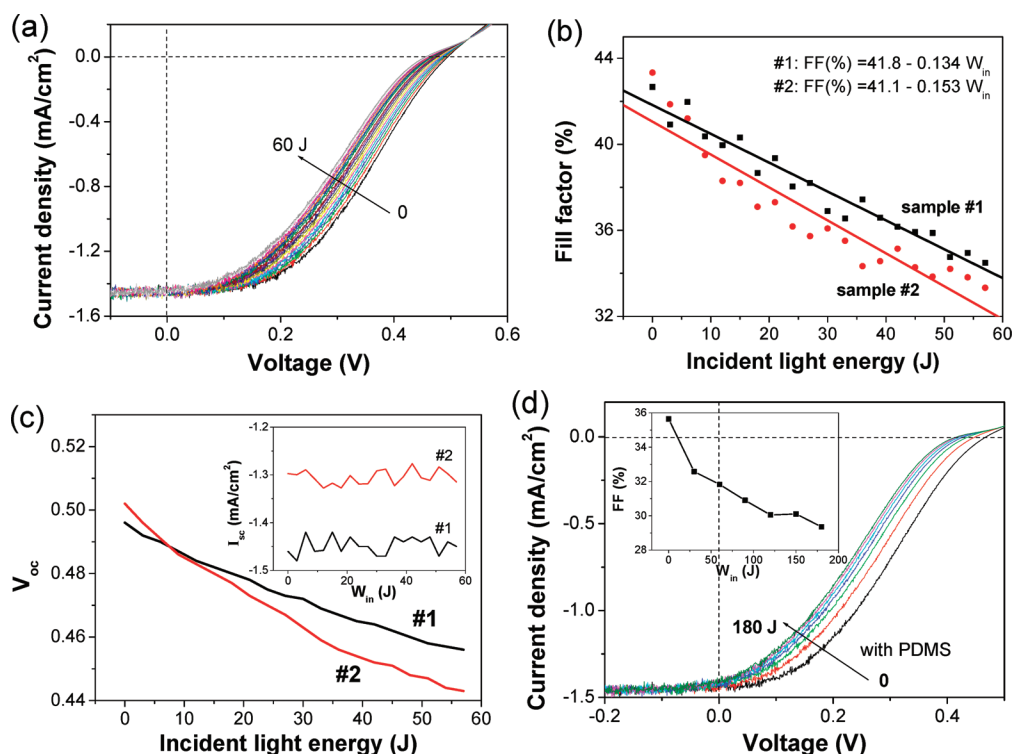


Figure 3. Linear dependence of fill factor and open-circuit voltage on the incident light energy. (a) A collection of 20 I - V curves from a CdS-SWNT-Si cell for every 1 min (corresponding to an incident light energy of 3 J) during a continuous 20 min illumination. (b) Plots of fill factors of two cell devices showing linear decrease from FF > 42% down to FF < 35% with increasing illumination time. (c) Plots of open-circuit voltages of the same two devices showing linear decrease from about 0.5 V to less than 0.46 V. Inset: plots of short-circuit current densities versus incident light energy (W_{in}). (d) I - V characteristics of a control sample (sealed with a PDMS film) showing similar shift of curves during continuous illumination. Inset shows the decrease of fill factor of the control sample.

and form an extra interface. However, here we mainly focus on the interaction between CdS and SWNTs and discuss the unique optoelectronic behavior of CdS-SWNT-Si cells.

The CdS-SWNT-Si solar cell with a 33 wt % of CdS nanoparticles shows an open-circuit voltage (V_{oc}) of 0.47 V, a short-circuit current density of 6.82 mA/cm² (I_{sc}), a fill factor (FF) of 43.7%, and a power conversion efficiency (η) of 1.4% (AM 1.5, 100 mW/cm²) (Figure 2a). Increasing the loading of CdS (e.g., 50 wt %) causes a shift of the I - V curve to the left, resulting in a reduced efficiency. This may be because nanoparticles reduce the interconnected nodes of the SWNT network and the SWNT-Si contact area. Control samples based on pure SWNTs show efficiencies up to 1.5%, indicating that a modest loading of CdS (<33 wt %) does not decrease the cell performance.

The I - V characteristics of CdS-SWNT-Si cells change systematically during continuous illumination. Figure 2b shows a series of I - V curves recorded every 10 min, in which the light energy received by each cell (up to 150 J) was calculated based on the active area, illumination time, and intensity. The fill factor of this cell has dropped monotonically from 42.3% (fresh sample) to less than 33% after 20 min of illumination (60 J) and then became stable (Figure 2c). The cell recovers to the original fill factor (43%) when placed in the dark for

6 h, and such reversible change is observed for many cycles. For comparison, a SWNT-Si control sample without CdS nanoparticles is very stable, maintaining a constant fill factor under prolonged illumination (Figure 2d).

The shift of I - V curves is quite uniform during a short period (less than 20 min) (Figure 3a). The decrease of fill factor exhibits a linear dependence on the incident light energy within a certain range (up to 60 J) (Figure 3b). Furthermore, the open-circuit voltage also drops linearly with increasing light energy, from about 0.5 V (pristine sample) down to less than 0.45 V (Figure 3c). In our cells, similar to that presented in the literature,²⁵ the open-circuit voltage may be associated with the built-in field at the interface of SWNTs and Si that mostly depend on the Fermi level difference between components of the solar cell. The reason for voltage change is unclear, although the electron doping of SWNTs could alter the built-in field. Meanwhile, another typical parameter, the short-circuit current, remains nearly constant with respect to incident energy (inset of Figure 3c). Such change of I - V characteristics has been observed in most of CdS-containing devices reproducibly, although the values of FF and V_{oc} vary slightly in different samples. The linear relationship between FF (as well as V_{oc}) and incident light energy is a useful property for constructing light sensors.

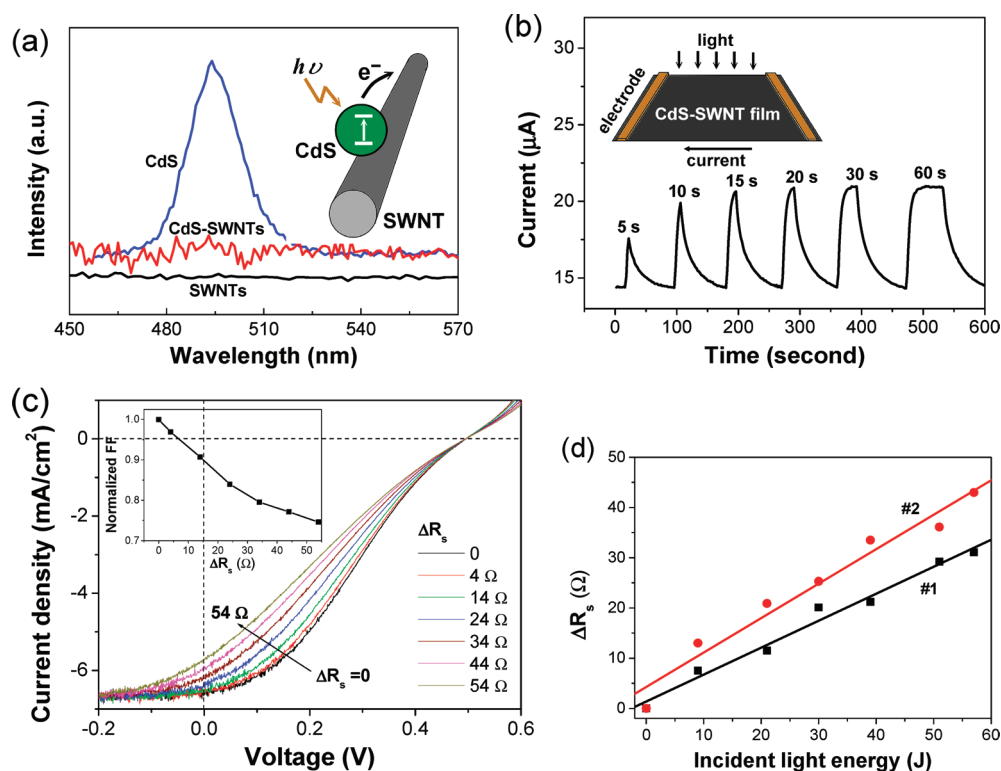


Figure 4. Mechanism study of the photoresponse behavior. (a) Fluorescence spectra of CdS nanoparticles (peak at 494 nm), SWNTs, and CdS-SWNT hybrids in which the emission of CdS is completely quenched. Inset: illustration of the electron transfer from the CdS particles to the SWNTs under light excitation. (b) Recorded current flow change of a CdS-SWNT hybrid film configured as a two-terminal device (illustrated in the inset) when incident light was turned on and off for time intervals of 5 to 60 s (corresponding to 0.25 to 3 J), respectively. (c) I - V characteristics recorded from a control sample (SWNT-Si cell) connected to additional series resistances increasing from 0 to 54 Ω . Inset: plot of normalized FF versus increased series resistance (ΔR_s). (d) Calculated relationship between the series resistance increase of CdS-SWNT-Si solar cells and incident light energy.

Light illumination may cause oxygen desorption (and readsorption) from SWNTs. We have removed this possibility by coating a transparent polydimethylsiloxane (PDMS) film onto the SWNT film to ensure that the top of cell device was fully sealed. As the SWNTs and CdS are not directly exposed to air, oxygen desorption due to illumination is inhibited. Interestingly, the PDMS-covered solar cell shows a shift of I - V curves and linear decrease of FF during testing similar to uncovered cells (Figure 3d). This indicates that the charge transfer between CdS and SWNTs (rather than oxygen desorption) is responsible for the reversible change of I - V characteristics of the hybrid film solar cells. Since CdS exists mainly as individual nanoparticles along the SWNT bundles (Figure 1d), the charge transfer between CdS particles with different sizes is minimal and has negligible effect on the cell performance compared with transfer between CdS and SWNTs. The charge-transfer process in similar hybrid systems has been studied in-depth by a few other groups.^{3,16} In our CdS-SWNT hybrid, the green-light fluorescence at 494 nm from CdS nanoparticles is completely quenched when they are grafted to SWNTs, confirming the strong CdS-SWNT interaction and electron flow under excitation (Figure 4a). In addition, we made a two-terminal device based on a CdS-SWNT film, which shows an ap-

preciable increase in current flow when exposed to light (Figure 4b). Notably, the current change saturates after about 30 s in the two-terminal contact structure, whereas light response (change of FF) in a solar cell configuration could continue for at least 20 min, as shown in Figure 2c. The hybrid films consisting of controlled band gap nanoparticles also have the potential to respond with different sensitivity to light intensity and wavelength, according to a recent report.¹³

We have measured a SWNT-Si cell by adding series resistors in the range of 4 to 54 Ω and observed that additional series resistance (R_s) causes a similar shift of I - V curves and drop in fill factor (Figure 4c). Considering solar cells in which the SWNT film acts as a hole transport path, the electron injection from CdS nanoparticles could reduce hole concentration, resulting in the increase of R_s and decrease of FF. The change of R_s (denoted as ΔR_s) in CdS-SWNT films due to charge transfer can be related to incident light energy based on the decrease of FF. For example, the value of FF has decreased by more than 25% with an additional R_s of 44 Ω (inset of Figure 4c), while FF dropped by 23% for a light energy of 60 J (Figure 2c). The increase of film resistance (ΔR_s) shows a linear dependence on incident energy to the CdS-SWNT-Si device, with a slope of 0.5–0.7 Ω /J (Figure 4d). By adding resistors to

SWNT–Si cells, we observe a constant V_{oc} and a decreasing I_{sc} as shown in Figure 4c, which is different from the behavior of CdS–SWNT–Si devices under continuous illumination. This implies that the increase of R_s (due to charge transfer between CdS and SWNTs) is not the only reason for the photoresponse of CdS–SWNT–Si cells.

In summary, we have fabricated solar cells with efficiencies $>1\%$ by constructing a hybrid film consisting of CdS-grafted SWNTs on a Si substrate. The fill factors and open-circuit voltages are tunable over a modest

range by light illumination. The CdS–SWNT–Si cells can be extended to include other types of nanotubes, such as double-walled and multiwalled tubes, or more semiconductor nanoparticles with unique electronic structures. It is also possible to explore the photoreponse of nanotube-on-Si solar cells to visible light as well as near-infrared by introducing selected nanoparticles with appropriate band gaps. The nanoparticle–nanotube hybrid materials have the potential to build innovative functional devices such as photovoltaics, sensors, and optical detectors.

EXPERIMENTAL SECTION

Preparation of CdS–SWNT Hybrid Films: Pristine SWNT material was provided by Prof. K. Jiang's group, which was prepared by chemical vapor deposition in the form of an aligned forest on a silicon substrate. CdS nanoparticles were synthesized using a procedure similar to that reported earlier.²⁶ CdS–SWNT hybrids were prepared via a noncovalent functionalization route as reported recently.²⁴ Thin films of CdS–SWNT hybrids were obtained by vacuum filtration, transfer to desirable substrates, and removal of filtration membrane (mixed cellulose ester membrane) using proper solvents. Here, the film thickness and size can be controlled by the solution volume and the membrane diameter. These hybrid films were then transferred to a patterned Si/SiO₂ wafer with a window size of 7×7 mm² where n-type silicon was exposed. The supporting membrane was completely removed by washing with a large quantity of solvents (acetone and toluene).

Sample Characterization and Device Testing. TEM characterization was performed using a LEO 912 Omega transmission electron microscope (Zeiss) at an accelerating voltage of 100 kV. SEM images were obtained using a Hitachi S-800 field emission scanning electron microscope (FESEM). Photoluminescence spectra were measured at room temperature using an ISS PC1 photon counting spectrofluorometer with an excitation wavelength of 370 nm. To make a solar cell device, a layer of Ti/Pd/Au with a total thickness of 100 nm was predeposited on the back side of n-type Si wafers before the deposition of CdS–SWNT hybrid films. Two thin copper wires were connected to the front (CdS–SWNT film) and back (Si coated with Ti/Pd/Au) electrodes via silver paint. The device was illuminated from the CdS–SWNT film side (as transparent electrode). Two types of control samples were made in our experiments. One is a cell device based on pure SWNT films without incorporating CdS nanoparticles. The other is a PDMS-covered device made by drop-casting PDMS solution onto the hybrid film and allowing the polymer to cure overnight. Solar cell I – V characteristics were tested by a solar simulator (Oriol 92250A-1000) equipped with Keithley 2400 under AM 1.5G condition at a calibrated intensity of 100 mW/cm². Photoresponse of solar cells was characterized by recording I – V data repeatedly (for example, at one minute intervals) under stable continuous illumination to obtain a series of I – V curves for comparison.

Acknowledgment. We thank Prof. Kaili Jiang from Tsinghua University for providing high-purity SWNT materials. X.L. acknowledges financial support from the College of Engineering, University of Hawaii at Manoa.

REFERENCES AND NOTES

- Georgakilas, V.; Gournis, D.; Tzitzios, V.; Pasquato, L.; Guldi, D. M.; Prato, M. Decorating Carbon Nanotubes with Metal or Semiconductor Nanoparticles. *J. Mater. Chem.* **2007**, *17*, 2679–2694.
- Wildgoose, G. G.; Banks, C. E.; Compton, R. G. Metal Nanoparticles and Related Materials Supported on Carbon Nanotubes: Methods and Applications. *Small* **2006**, *2*, 182–193.
- Robel, I.; Bunker, B. A.; Kamat, P. V. Single-Walled Carbon Nanotube–CdS Nanocomposites as Light-Harvesting Assemblies: Photoinduced Charge-Transfer Interactions. *Adv. Mater.* **2005**, *17*, 2458–2463.
- Juárez, B. H.; Klinke, C.; Kornowski, A.; Weller, H. Quantum Dot Attachment and Morphology Control by Carbon Nanotubes. *Nano Lett.* **2007**, *7*, 3564–3568.
- Hwang, S.-H.; Moorefield, C. N.; Wang, P.; Jeong, K. U.; Cheng, S. Z. D.; Kotta, K. K.; Newkome, G. R. Dendron-Tethered and Template CdS Quantum Dots on Single-Walled Carbon Nanotubes. *J. Am. Chem. Soc.* **2006**, *128*, 7505–7509.
- Li, X.; Liu, Y.; Fu, L.; Cao, L.; Wei, D.; Yu, G.; Zhu, D. Direct Route to High-Density and Uniform Assembly of Au Nanoparticles on Carbon Nanotubes. *Carbon* **2006**, *44*, 3139–3142.
- Li, X.; Liu, Y.; Fu, L.; Cao, L.; Wei, D.; Wang, Y. Efficient Synthesis of Carbon Nanotube–Nanoparticle Hybrids. *Adv. Funct. Mater.* **2006**, *16*, 2431–2437.
- Correa-Duarte, M. A.; Liz-Marzán, L. M. Carbon Nanotubes as Templates for One-Dimensional Nanoparticle Assemblies. *J. Mater. Chem.* **2006**, *16*, 22–25.
- Grzelczak, M.; Correa-Duarte, M. A.; Salgueiriño-Maceira, V.; Giersig, M.; Diaz, R.; Liz-Marzán, L. M. Photoluminescence Quenching Control in Quantum Dot–Carbon Nanotube Composite Colloids Using a Silica-Shell Spacer. *Adv. Mater.* **2006**, *18*, 415–420.
- Lu, C.; Akey, A.; Wang, W.; Herman, I. P. Versatile Formation of CdSe Nanoparticle–Single Walled Carbon Nanotube Hybrid Structures. *J. Am. Chem. Soc.* **2009**, *131*, 3446–3447.
- Mu, Y.; Liang, H.; Hu, J.; Jiang, L.; Wan, L. Controllable Pt Nanoparticle Deposition on Carbon Nanotubes as an Anode Catalyst for Direct Methanol Fuel Cells. *J. Phys. Chem. B* **2005**, *109*, 22212–22216.
- Matsumoto, T.; Komatsu, T.; Arai, K.; Yamazaki, T.; Kijima, M.; Shimizu, H.; Takasawa, Y.; Nakamura, J. Reduction of Pt Usage in Fuel Cell Electrocatalysts with Carbon Nanotube Electrodes. *Chem. Commun.* **2004**, 840–841.
- Kang, Y.; Kim, D. Enhanced Optical Sensing by Carbon Nanotube Functionalized with CdS Particles. *Sens. Actuators, A* **2006**, *125*, 114–117.
- Sun, Y.; Wang, H. H. Electrodeposition of Pd Nanoparticles on Single-Walled Carbon Nanotubes for Flexible Hydrogen Sensors. *Appl. Phys. Lett.* **2007**, *90*, 213107-1–213107-3.
- Zhu, Y.; Elim, H. I.; Foo, Y. L.; Yu, T.; Liu, Y.; Ji, W.; Lee, J. Y.; Shen, Z.; Wee, A. T.-S.; Thong, J. T.-L.; Sow, C.-H. Multiwalled Carbon Nanotubes Beaded with ZnO Nanoparticles for Ultrafast Nonlinear Optical Switching. *Adv. Mater.* **2006**, *18*, 587–592.
- Hu, L.; Zhao, Y. L.; Ryu, K.; Zhou, C.; Stoddart, J. F.; Grüner, G. Light-Induced Charge Transfer in Pyrene/CdSe–SWNT Hybrids. *Adv. Mater.* **2008**, *20*, 939–946.
- Kymakis, E.; Amaratunga, G. A. J. Single-Wall Carbon Nanotube/Conjugated Polymer Photovoltaic Devices. *Appl. Phys. Lett.* **2002**, *80*, 112–114.

18. Kalita, G.; Adhikari, S.; Aryal, H. R.; Umeno, M.; Afre, R.; Soga, T.; Sharon, M. Cutting Carbon Nanotubes for Solar Cell Application. *Appl. Phys. Lett.* **2008**, *92*, 123508-1–123508-3.
19. Landi, B. J.; Castro, S. L.; Ruf, H. J.; Evans, C. M.; Bailey, S. G.; Raffaele, R. P. CdSe Quantum Dot–Single Wall Carbon Nanotube Complexes for Polymeric Solar Cells. *Sol. Energy Mater. Sol. Cells* **2005**, *87*, 733–746.
20. Landi, B. J.; Raffaele, R. P.; Castro, S. L.; Bailey, S. G. Single-Wall Carbon Nanotube–Polymer Solar Cells. *Prog. Photovoltaics* **2005**, *13*, 165–172.
21. Kanai, Y.; Grossman, J. C. Role of Semiconducting and Metallic Tubes in P3HT/Carbon-Nanotube Photovoltaic Heterojunctions: Density Functional Theory Calculations. *Nano Lett.* **2008**, *8*, 908–912.
22. Wei, J.; Jia, Y.; Shu, Q.; Gu, Z.; Wang, K.; Zhuang, D.; Zhang, G.; Wang, Z.; Luo, J.; Cao, A.; Wu, D. Double-Walled Carbon Nanotube Solar Cells. *Nano Lett.* **2007**, *7*, 2317–2321.
23. Jia, Y.; Wei, J.; Wang, K.; Cao, A.; Shu, Q.; Gui, X.; Zhu, Y.; Zhuang, D.; Zhang, G.; Ma, B.; Wang, L.; Liu, W.; Wang, Z.; Luo, J.; Wu, D. Nanotube–Silicon Heterojunction Solar Cells. *Adv. Mater.* **2008**, *20*, 4594–4598.
24. Li, X.; Jia, Y.; Cao, A. Tailored Single-Walled Carbon Nanotube–CdS Nanoparticle Hybrids for Tunable Optoelectronic Devices. *ACS Nano* **2010**, *4*, 506–512.
25. Li, Z.; Kunets, V. P.; Saini, V.; Xu, Y.; Dervishi, E.; Salamo, G. J.; Biris, A. R.; Biris, A. S. SOCl_2 Enhanced Photovoltaic Conversion of Single Wall Carbon Nanotube/n-Silicon Heterojunctions. *Appl. Phys. Lett.* **2008**, *93*, 243117-1–243117-3.
26. Yong, K.; Sahoo, Y.; Swihart, M. T.; Prasad, P. N. Shape Control of CdS Nanocrystals in One-Pot Synthesis. *J. Phys. Chem. C* **2007**, *111*, 2447–2458.